Chemical Engineering Journal 193–194 (2012) 21–30

Contents lists available at SciVerse ScienceDirect

Chemical Engineering Journal

journal homepage: www.elsevier.com/locate/cej

Equilibrium and kinetic study of arsenic sorption by water-insoluble nanocomposite resin of poly[*N*-(4-vinylbenzyl)-*N*-methyl-D-glucamine]-montmorillonite

Bruno F. Urbano [a], Bernabé L. Rivas [a,*], Francisco Martinez [b], Spiro D. Alexandratos [c]

[a] Departamento de Polímeros, Facultad de Ciencias Químicas, Universidad de Concepción, Casilla 160-C, Concepción, Chile
[b] Departamento de Ciencias de los Materiales, Facultad de Ciencias Físicas y Matemáticas, Universidad de Chile, Casilla 2777, Santiago, Chile
[c] Department of Chemistry, Hunter College of the City University of New York, 695 Park Avenue, New York, NY 10065, United States

ARTICLE INFO

Article history:
Received 17 December 2011
Received in revised form 23 March 2012
Accepted 23 March 2012
Available online 11 April 2012

Keywords:
Arsenic
Adsorption
N-methyl-D-glucamine
Kinetic
Ion exchange
Isotherms

ABSTRACT

This research presents the kinetic and equilibrium performance of arsenic sorption by a novel polymer-clay nanocomposite ion exchange resin. The monomer *N*-(4-vinylbenzyl)-*N*-methyl-D-glucamine was previously synthesised and subsequently polymerised via radical initiation in the presence of crosslinking reagent *N,N*-methylene-*bis*-acrylamide and organic-modified montmorillonite. The sorption of arsenic(V) was studied as a function of time, initial concentration and pH. Experiments as a function of pH revealed that arsenic sorption was favoured in the pH range from 3 to 6. The experimental data were fitted to kinetic and diffusion models, such as pseudo-first order, pseudo-second order, Elovich, and the intra-particle diffusion model. The pseudo-second order model presented the best correlation with the experimental data. The model indicated that high percentages of retention could be achieved in a short time (>90%, 1 h of contact) at pH 6 when the initial arsenic concentration was between 5 and 50 mg/L. Intra-particle diffusion and the Boyd relationship showed that arsenic sorption was controlled by the film diffusion mechanism. The Langmuir, Freundlich, and Dubinin–Radushkevitch isotherms were fitted to experimental data, and the Langmuir isotherm presented the best fit. Thermodynamic parameters ($\Delta G°$, $\Delta H°$, $\Delta S°$) showed that the arsenic sorption process was a spontaneous process, endothermic, and produced an increase in entropy.

1. Introduction

Water plays important roles in human activities, the natural environment, and social development. One of the most important problems in water use is arsenic pollution due to its high toxicity. Arsenic pollution concerns the entire world, particularly in countries where water naturally has high arsenic concentrations, such as Bangladesh, India, China, Chile, Argentina, and Mexico [1]. The World Health Organization (WHO) and the Environmental Protection Agency (EPA) have strictly reduced the maximum contaminant level recommended from 50 μg/L to 10 μg/L to minimise the risk to humans [2]. Therefore, it is necessary to research new sorption procedures able to remove arsenic selectively.

Arsenic exists in water primarily as arsenate, As(V), and arsenite, As(III), in the forms of arsenic acid (H_3AsO_4) and arsenous acid (H_3AsO_3), respectively. The arsenic species are pH dependent and the most dominant species in natural waters is the monovalent oxyanion ($H_2AsO_4^-$). Several technologies exist for arsenic removal, such as coagulation-precipitation, filtration, and adsorption [3], with adsorption being the most extensively studied because it has better performance, easier operation, lower cost and the possibility to recycle [4–7].

Ion exchange resins containing *N*-methyl-D-glucamine (NMDG) are widely used for selective boron removal [8,9]. This ligand has also been studied for oxyanion uptake of molybdate, vanadate, chromate, and arsenate [10,11]. Arsenic uptake presented the most promising results, and it has been demonstrated that ion exchange resins containing NMDG ligands improve the retention of arsenate as $H_2AsO_4^-$ at pH 4–6. Additionally, the NMDG ligand showed a high selectivity toward arsenate ions, even in the presence of a high concentration of sulphate [12,13].

The development of new materials for potential application in ion exchange has presented important advances. These have included solvent impregnated resins and metal-loaded ion exchange resins, which consist of hybrid materials to obtain new materials with improved properties [14–17]. Our group has reported the synthesis of polymer-clay nanocomposites of monomers able to interact with metal ions and loaded with organic-modified montmorillonite. The nanocomposites presented enhanced mechanical

* Corresponding author. Fax: +56 41 2245974.
E-mail address: brivas@udec.cl (B.L. Rivas).

1385-8947/$ - see front matter © 2012 Elsevier B.V. All rights reserved.
http://dx.doi.org/10.1016/j.cej.2012.03.065

Nomenclature

C	Intercept intra-particle diffusion model (mg/g_{resin})
C_0	Initial solute concentration (mg/L)
C_{eq}	Equilibrium solute concentration (mg/L)
D_p	Pore diffusion coefficient (cm^2/min)
E	Free energy of adsorption (kJ/mol)
h	Initial solute adsorption (mg/gresin min)
k_1	Pseudo-first order constant rate (1/min)
k_2	Pseudo-second order constant rate (g_{resin}/mg min)
k_{DR}	Dubinin–Radushkevitch isotherm constant
k_f	Freundlich constant
k_{ip}	Intra-particle rate constant (g_{resin}/mg $min^{0.5}$)
k_L	Langmuir constant (L/mg)
MBA	Methylene-*bis*-acrylamide
MMT	Montmorillonite
n	Freundlich parameter, dimensionless
NMDG	*N*-methyl-D-glucamine
PVbNMDG	Poly[*N*-(4-vinylbenzyl)-*N*-methyl-D-glucamine]
q_e	Equilibrium adsorption capacity (mg/g_{resin})
q_m	Monolayer capacity (mg/g_{resin})
q_t	Adsorption capacity at time t (mg/g_{resin})
r^2	Correlation coefficient
R_L	Langmuir separation factor
t	Time of adsorption (min)
VBC	4-vinylbenzyl chloride
VbNMDG	*N*-(4-vinylbenzyl)-*N*-methyl-D-glucamine
α	Elovich initial adsorption rate (mg min/g_{resin})
β	Elovich surface coverage parameter (g resin/mg)
ΔG°	Gibbs free energy change (kJ/mol)
ΔH°	Enthalpy change (kJ/mol)
ΔS°	Entropy change (kJ/mol)
ε	Polanyi potential

properties through the addition of montmorillonite and further studies showed favourable metal-ion retention properties [18].

The aim of this paper was the study of arsenic sorption properties using a novel nanocomposite ion exchange resin consisting of a polymeric matrix bearing *N*-methyl-D-glucamine. This research emphasised the kinetic and equilibrium characteristics of arsenic sorption. Equilibrium studies provide useful information about the affinity or capacity of the adsorbent, while kinetic studies provide information on the time needed to accomplish the sorption process and how sorption rate depends on the concentration of the solute and the characteristics of the adsorbent [19]. Polymer-clay nanocomposite resins were obtained by *in situ* radical polymerisation of a monomer based on *N*-methyl-D-glucamine in the presence of *N*-methylene-*bis*-acrylamide and organic-modified montmorillonite as crosslinking and filler reagents, respectively. The monomer based on the NMDG ligand is not commercially available and was thus synthesised. The sorption of arsenate was evaluated as a function of time, and the experimental data were fitted using both kinetic and diffusion models to obtain information on the sorption process. In addition, equilibrium batch studies were carried out, and thermodynamic parameters were calculated.

2. Experimental procedure

2.1. Materials

The monomer *N*-(4-vinylbenzyl)-*N*-methyl-D-glucamine (VbNMDG) was synthesised using the precursors 4-vinylbenzyl chloride (VBC, Aldrich) and *N*-methyl-D-glucamine (NMDG, Aldrich) as received. The reagent *N,N*-methylene-*bis*-acrylamide (MBA, 98%, Aldrich) and ammonium persulphate (Aldrich) were used as crosslinker and initiator reagents, respectively. Dihydrogen sodium arsenate heptahydrate salt (99%, Aldrich) was used to prepare arsenic solutions for the sorption experiments. Montmorillonite K10 (CEC 70–120 meq/100 g, Aldrich) $[M_y^+(Al_{2-y}Mg_y)(Si_4)\ O_{10}(OH)_2 * nH_2O]$ previously modified using 3-acrylamidopropyl(trimethylammonium) chloride (Aldrich) was used as filler.

2.2. Synthesis

2.2.1. Synthesis of N-(4-vinylbenzyl)-N-methyl-D-glucamine monomer

In a three necked round bottomed flask, the reaction of *N*-methyl-D-glucamine and 4-vinylbenzyl chloride was carried out in a mole ratio of 1:1. Reagent grade *N*-methyl-D-glucamine (21.9 mmol) was dissolved in a 2:1 volume solvent mixture of dioxane and deionised water. The solution was added to the reactor and heated for 20 min until NMDG was completely dissolved. Next, 3.20 mL (21.9 mmol) of 4-vinylbenzyl chloride was dissolved in 10 mL of dioxane and slowly added to the reactor. The reaction was kept under reflux with constant stirring for 5 h, and a yellow solution was obtained. To remove unreacted VBC, the solution was washed with ethyl ether twice.

2.2.2. Montmorillonite modification

Montmorillonite was modified to improve the interaction of polymeric matrix with the clay surface. Organic-modified montmorillonite was obtained by a previously reported experimental procedure [18]. Briefly, 5.0 g of Na^+-montmorillonite was dispersed in 200 mL of distilled water and an excess of intercalating agent (3-acrylamidepropyl)trimethylammonium chloride was added. The mixture was stirred for 24 h at 30 °C. Organic-modified montmorillonite was filtered and washed with an excess of distilled water until no chloride ion was detection by $AgNO_3$. Finally, the clay was dried in an oven at 40 °C.

2.2.3. Poly[N-(4-vinylbenzyl)-N-methyl-D-glucamine]-MMT nanocomposite synthesis

Water-insoluble nanocomposite resins were synthesised by *in situ* radical polymerisation. The solution of *N*-(4-vinylbenzyl)-*N*-methyl-D-glucamine monomer was added to a polymerisation tube. Subsequently, the crosslinker reagent *N,N*-methylene-*bis*-acrylamide (4 mol% with respect to the monomer) and the organic-modified montmorillonite (2.5 wt.% with respect to the monomer) were added. Finally, the radical initiator benzoyl peroxide (2 mol%) was added to the reactor, and the mixture was degassed with nitrogen gas for 10 min. The reaction was stirred for 4 h under a nitrogen atmosphere at 75 °C. Resins were extracted and washed with dioxane, distilled water, and dried in an oven at 50 °C.

2.3. Physicochemical characterisation

Evaluation of the functional groups present on the resins was carried out by Fourier transformed infrared spectroscopy (FTIR) on a Perkin Elmer 1760-X spectrometer from 4000 to 400 cm^{-1} using KBr pellets. The interlayer distances of raw montmorillonite, organic-modified and montmorillonite dispersed within nanocomposites were determined by X-ray diffraction in a RIGAKU, Geigerflex model diffractometer (CuKα tube, 40 kV, 20 mA) in the range of 2–15° 2θ at 1°/min. Transmission electron microscopy (TEM)

analysis was performed to evaluate the nanocomposite morphology and to obtain direct and visual information on the dispersed clays. For this purpose, the nanocomposite resins were analysed with a JEOL/JEM 1200 EX II instrument. Scanning electron microscopy (SEM) was performed in a SEM-PROBE CAMECA, model SU-30, to evaluate the surface characteristics of the resins. The arsenic concentrations were measured using a Unicam solar atomic absorption spectrometer equipped with a hydride generator (quantification limit of 1.07 μg/L).

2.4. Arsenate sorption experiments

Batch equilibrium experiments were performed to evaluate the arsenate retention by nanocomposite resins. Sieved dry resins of particle size fraction between 180 and 250 μm were used for all sorption experiments.

The effect of pH on retention was studied to obtain a correlation between arsenic speciation and sorption performance of nanocomposite resins. Experiments were carried out using a batch procedure at 25 °C, 140 rpm, and over 24 h. Arsenic aqueous solutions were adjusted to a pH of 2.0–12.0 (±0.1) using dilute nitric acid and sodium hydroxide solutions. All experiments were carried out in a contact tube using 30 mg of PVbNMDG nanocomposite resin and 5 mL of arsenic solution placed in a shaker equipped with a thermoregulated bath at 25 °C and 140 rpm over 24 h. Afterwards, mixtures were filtered and collected in a calibrated flask for further measurement of arsenic concentration.

2.5. Equilibrium and kinetic studies

Equilibrium sorption experiments were performed by the batch procedure. In a contact tube, 30 mg of nanocomposite resin was combined with 5 mL of arsenate solution at 30, 40, and 50 °C at 140 rpm over 30 h. The experiments were carried out at pH 6.0 using the same dose of nanocomposite resin (30 mg) and varying the arsenic concentration (range of 1–700 mg/L). After contact, resins were filtered, washed, and arsenic concentrations were determined by atomic absorption spectroscopy. The amount of arsenate species retained was determined by the difference from the initial concentration.

The sorption of arsenic as a function of time was studied at pH 3.0 and 6.0 at three concentrations between 5 and 200 mg/L. Experiments were performed between 0 and 24 h of contact at 25 °C and 140 rpm. The same resin dose and volume of arsenic solution were used in these equilibrium studies. The contact tubes were withdrawn from the shaker at different time intervals and the resins were handled as described above.

3. Results and discussion

3.1. Nanocomposite characterisation

3.1.1. Infrared spectroscopy

Fig. 1 shows the infrared spectra of raw montmorillonite (MMT) and organic-modified (OMMT). The montmorillonite spectrum presents characteristic vibrational bands at 3643 cm^{-1} (O–H st), 3347 cm^{-1} (H_2O st), and 1034 cm^{-1} (Si–O st). For modified montmorillonite, the spectrum presents both MMT and (3-acrylamidopropyl)trimethylammonium chloride characteristic bands at 3046 cm^{-1} (C═C st), 1670 cm^{-1} (C═O st), and 1490 cm^{-1} (N^+–H st). In addition, Fig. 1 shows the infrared spectra of poly(*N*-(4-vinylbenzyl)-*N*-methyl-D-glucamine) nanocomposite loaded with 2.5% modified montmorillonite. The spectrum presents the characteristic vibration bands of both precursors used: 1084 cm^{-1} ν(C–O) and 1035 cm^{-1} ν(C–N), corresponding with vibrations of

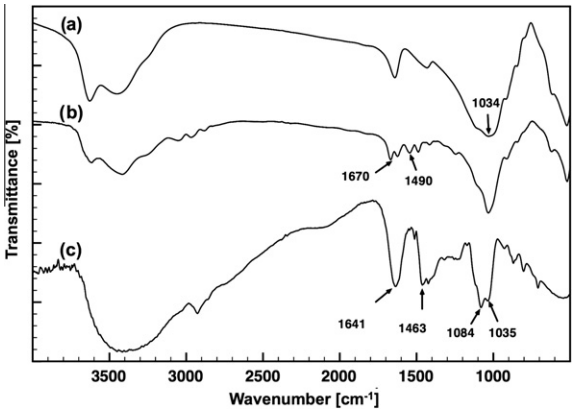

Fig. 1. Infrared spectra of (a) raw montmorillonite (MMT), (b) organic modified montmorillonite (OMMT) and (c) PVbNMDG - 2.5%OMMT.

N-methyl-D-glucamine, and bands at 1463 cm^{-1} ν(CH_2) and 1641 cm^{-1} ν(C═C) related to the 4-vinylbenzyl chloride monomer. Note that the stretching band associated to Si–O of clays did not appear due to the low content in the nanocomposite. The characteristic vibrational band related to the stretching of C–Cl at 1270 cm^{-1} of the 4-vinylbenzyl chloride monomer did not appear in the resin spectrum, indicating that the reaction between NMDG and VBC occurred and that the *N*-methyl-D-glucamine was attached to the polymeric matrix.

3.1.2. X ray diffraction and electron microscopy

The morphology of the nanocomposites was studied by X-ray diffraction and scanning electron microscopy. The former gives information related to the interlayer distance between the layers of montmorillonite and provides information on the morphology (exfoliated, intercalated, or tactoid clay layers). The latter technique gives information on the surface of the nanocomposite and its characteristics. Fig. 2 shows the X-ray diffraction patterns for different stages of nanocomposite synthesis. The pattern of raw montmorillonite shows its characteristic peak associated to plane d001. Once the montmorillonite was modified with (3-acrylamidopropyl)trimethylammonium chloride, the pattern showed a new peak at lower angles (∼5.7° 2θ), indicating that the interlayer distance increased as a consequence of incorporating the intercalating agent. However, the original peak of montmorillonite was still present in the pattern, suggesting that the intercalation process was not complete. Fig. 2 shows the XRD pattern of montmorillonite dispersed within the polymeric matrix. The pattern did not present

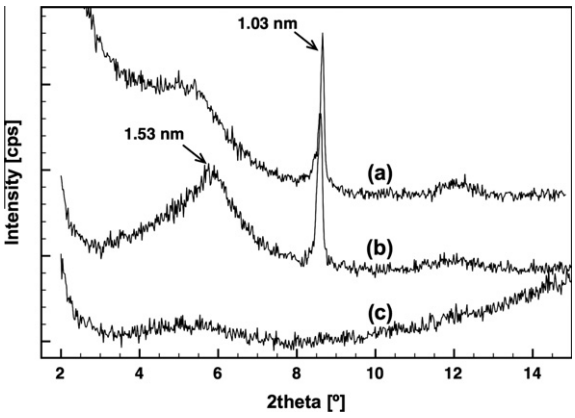

Fig. 2. XRD patterns for (a) raw montmorillonite, (b) organic modified montmorillonite and (c) PVbNMDG-2.5% OMMT.

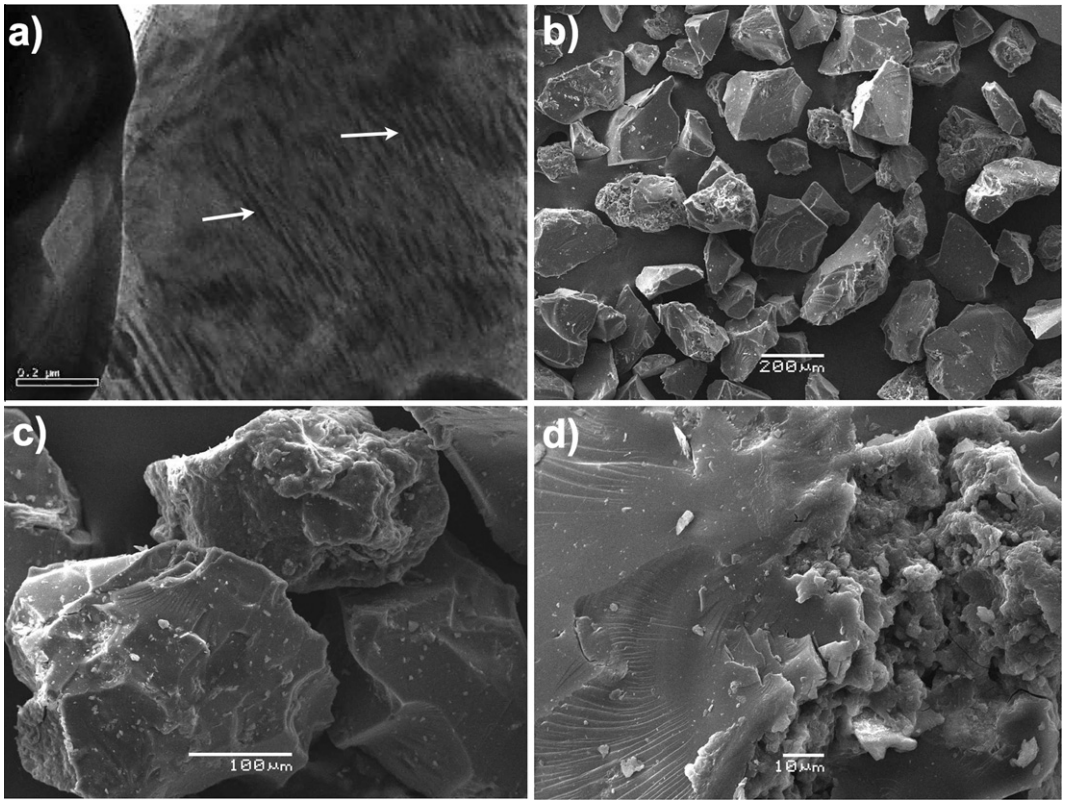

Fig. 3. Scanning electron images of PVbNMDG nanocomposite loaded with 2.5% of montmorillonite.

defined peaks, but an increase in diffraction intensity between 3° and 8° 2θ (broad peak) with a maximum at the same angle of the OMMT diffraction peak was observed. Hence, it was possibly to conclude that the resin possessed a certain degree of intercalated morphology.

Transmission electron microscopy images provided visual conformation that the clays were dispersed within the PVbNMDG resins (Fig. 3a). The dark lines observed in the micrographs corresponded to dispersed clay layers, and according to the scale, they were dispersed at the nano level. Scanning electron microscopy gives information on the surface and shape of resin particles. It was thus possible to observe in Fig. 3b that the resin particles possessed an irregular shape, while in Fig. 3c and d, the particles were porous and rough. In the other zones, the surface was uniform and smooth.

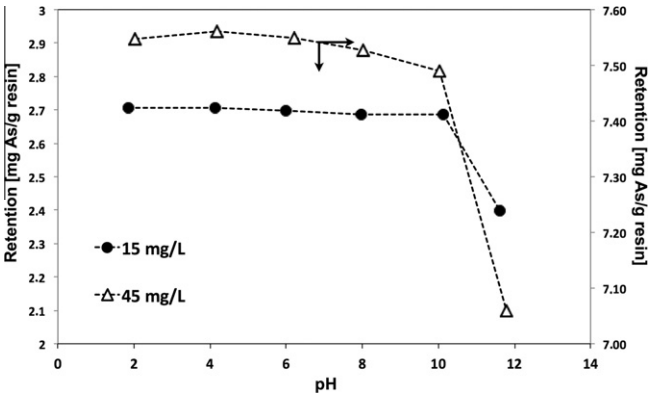

Fig. 4. Effect of pH on arsenic sorption by PVbNMDG nanocomposite.

3.2. Effect of pH on sorption

The pH is a key factor in obtaining good performance in several sorption processes, especially ion exchange. Hydronium in water can change the structural properties of ligands of resins and also the speciation of metal ions in aqueous solution, affecting sorption. Fig. 4 shows the effect of pH on arsenate sorption studied with a batch equilibrium procedure for two arsenic concentrations. Both curves present a similar trend in which arsenate retention remained static up to pH 8, where retention began to decrease. The maximum retention was observed between pH 3 and 6, where arsenic is found primarily as $H_2AsO_4^-$. The main characteristic of *N*-methyl-D-glucamine as ligand was the interaction of monovalent arsenate species with the protonated tertiary amine [12]. In contrast, strongly basic anion exchange resins with ammonium groups interact better with divalent species of arsenic ($H_2AsO_4^-$) in the pH range of 8–10 [20].

The maximum retention capacity experiments were carried out at pH 3 and 6 using a high arsenic concentration (1.2 g/L) to saturate the resin. The pH values were chosen according to the literature and previous results obtained by our group. The result showed that retention capacity was higher at pH 6 than pH 3 reaching 73.01 and 66.96 mg As/g_{resin}, respectively.

3.3. Sorption kinetics

The evaluation of the kinetics of the sorption process was an important issue before scaling up to industrial process scale. In this study, kinetic experiments were carried out by the batch procedure for a period of 24 h. Experiments used different concentrations of arsenic and the effect of pH was evaluated (pH 3–6) and compared with the results obtained above (Section 3.2).

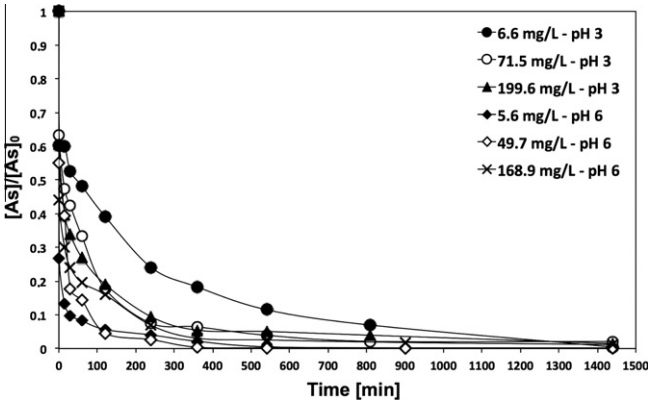

Fig. 5. Effect of time on arsenic sorption by PVbNMDG resin.

Several kinetic models have been used to determine the rate constants of different systems. Widely used kinetic models are those based on the decrease of available active sites to interact with solute (adsorption capacity) and have been successfully used to determine rate constants and characteristics of the sorption process (e.g., pseudo-first order model [21], pseudo-second order model [22], Elovich equation [23]). The term "pseudo" is used to distinguish the use of solute concentration from solid concentrations [24].

Fig. 5 presents the change of arsenic concentration as a function of time. It was observed that nanocomposite resins adsorbed a high amount of arsenic in a short period of time, especially for those experiments carried out at pH 6. After 1 h of contact, the experiments with initial arsenic concentrations of 5.6, 49.7 and 168.9 mg/L had adsorbed 91.7%, 85.6% and 80.5%, respectively. On the other hand, for experiments at pH 3, the percentages of retention were 51.8%, 66.7% and 73.1% for 6.6, 71.5 and 199.6 mg/L, respectively. The differences in uptake percentage could be explained by the speciation of arsenate in aqueous media. At pH 6, a major amount of arsenate exists in the monovalent form ($H_2AsO_4^-$), and based on our previous results and the literature, it has been demonstrated that sorption is favoured at pH 6 [12,25].

3.3.1. Elovich model

The Elovich equation is one of the first equations used for the chemisorption process and is mostly used for highly heterogeneous systems [23,26]. The model assumes a decrease in adsorption rate with an increase in adsorbed solute, and its linear form is expressed by Eq. (1):

$$q_t = \frac{1}{\beta}\ln(\alpha\beta) + \frac{1}{\beta}\ln(t) \quad (1)$$

where α (mg min/g) is the initial sorption rate and β (g/mg) is a parameter related to the extent of surface coverage and activation energy for chemisorption. Table 1 presents the kinetic parameters obtained from the Elovich model fitted to experimental data. The correlation coefficients are higher than pseudo-first order and lower than pseudo-second order (except to C_0 = 49.7 mg/L). Additionally, it was possible to observe that the initial sorption rate was related to arsenic concentration. For experiments carried out at pH 3, as the initial concentration increased the parameter α also increased. It was interesting that the high initial rate observed for an arsenic concentration of 5.6 mg/L, the value was ten orders of magnitude higher than the experiment carried out at pH 3 (C_0 = 6.6 mg/L). This was in agreement with the trend observed in Fig. 5, where the curve for pH 6 and 5.6 mg/L presented the sharpest drop, indicating a higher initial sorption compared with the rest of the experiments.

3.3.2. Pseudo-first order model

Lagergren proposed the pseudo-first order model for describing the adsorption process of solid-liquid systems and its linear form is formulated below:

$$\log(q_e - q_t) = \log(q_e) - \frac{k_1}{2.303}t \quad (2)$$

where q_e (mg/g_{resin}) and q_t are the amounts of arsenic adsorbed at equilibrium and at time t, respectively. The slope from a plot of $\log(q_e - q_t)$ vs. t allows determination of the rate constant k_1 (1/min). Fig. 6 shows the curves obtained fitting the model and Table 1 summarises the corresponding values associated to pseudo-first order parameters for the experimental data. The curves presented in Fig. 6 illustrate the poor fit of the model with the experimental data, which was confirmed by the correlation values. However, the pseudo-first order model was useful to describe the initial sorption periods. The deviation observed could be attributed to the sharp fall in gradient concentration as a consequence of a high initial arsenic sorption. The values for equilibrium sorption calculated by the model were quite different from those values obtained experimentally, indicating that this model was not appropriated to describe the sorption of arsenic by a PVbNMDG nanocomposite.

Table 1
Kinetic parameters for pseudo-first order, pseudo-second order and Elovich models.

	C_0 As (mg/L) – pH 3			C_0 As (mg/L) – pH 6		
	6.6	71.5	199.6	5.6	49.7	168.9
$q_{e,exp}$ (mg As/g_{resin})	1.10	11.91	33.27	0.94	8.28	28.13
Pseudo-First order						
$q_{e,cal}$ (mg As/g_{resin})	0.61	6.42	10.84	0.12	1.84	6.97
$k_1 \times 10^{-3}$ (1/min)	2.76	8.06	3.91	5.06	9.21	4.83
r^2	0.9816	0.9594	0.8618	0.9506	0.9023	0.9109
Pseudo-second order						
$q_{e,cal}$ (mg As/g_{resin})	1.11	11.83	33.00			
	0.94	8.31	28.11			
$k_2 \times 10^{-3}$ (g_{resin}/mg As min)	17.1	4.74	1.76	207.2	19.69	3.247
h (mg As/g_{resin} min)	0.021	0.66	1.92	0.183	1.359	2.566
r^2	0.9957	0.9997	0.9996	0.9999	0.9999	0.9998
Elovich equation						
α (mg As min/g_{resin})	0.144	10.591	173.71	7.68×10^9	686.08	4332.52
β (g_{resin}/mg As)	6.506	0.7405	0.33	35.587	1.6162	0.5188
r^2	0.9844	0.9321	0.9624	0.9743	0.7781	0.9528

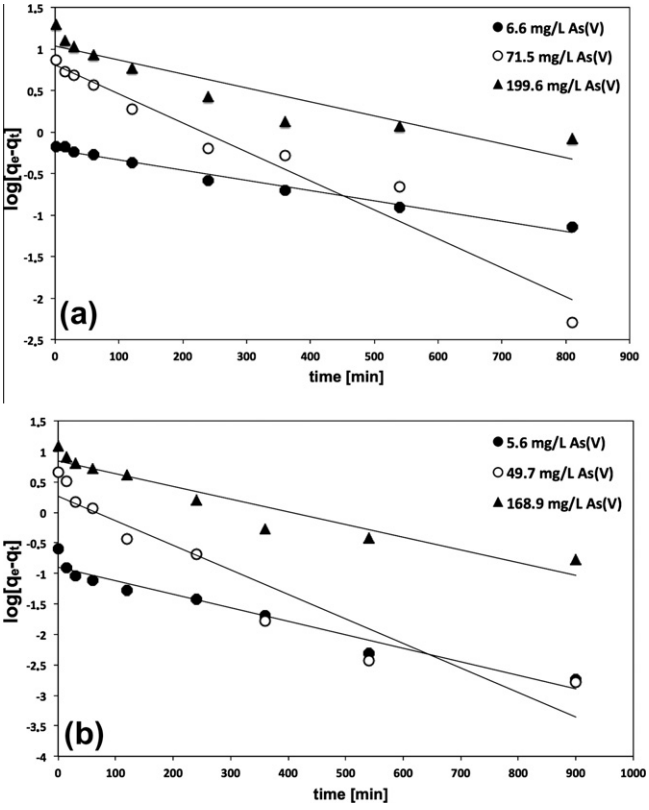

Fig. 6. Lagergren pseudo-first order model for arsenic sorption, as function of initial arsenic concentration at (a) pH 3 and (b) pH 6.

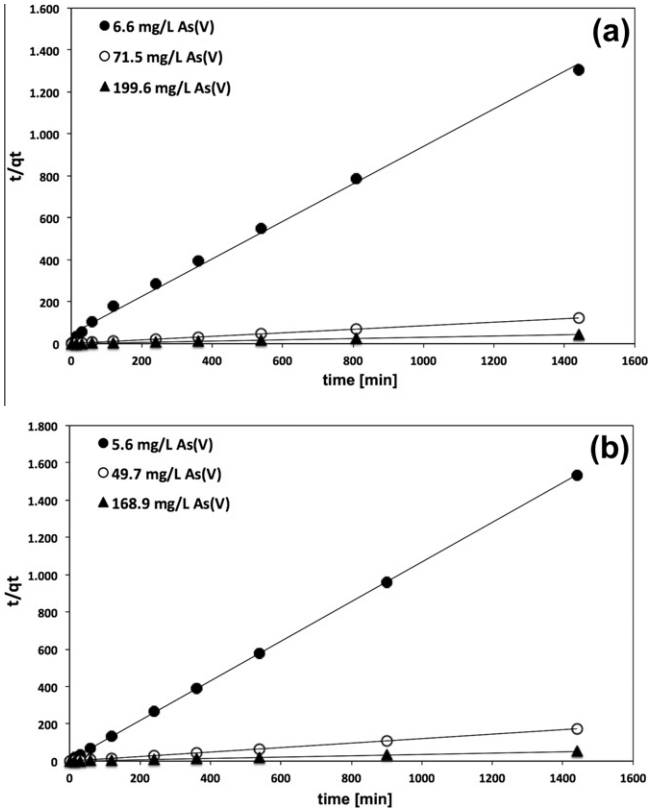

Fig. 7. Pseudo-second order linear plots for arsenic sorption, as function of initial concentrations of arsenic at (a) pH 3 and (b) pH 6.

3.3.3. Pseudo-second order model

The pseudo-second order equation has been widely used due the excellent fit of experimental data for the entire sorption period of many systems [22]. The kinetic model can be expressed as shown below:

$$\frac{dq_t}{dt} = k_2(q_e - q_t)^2 \tag{3}$$

Integrating and assuming boundary conditions, the rearranged linear form of the pseudo-second order model is obtained:

$$\frac{t}{q_t} = \frac{1}{k_2 q_e^2} + \frac{t}{q_e} \tag{4}$$

where q_e and q_t are the arsenic amounts adsorbed (mg/g_{resin}) at equilibrium and at time t, respectively, $h = kq_e^2$ is the initial sorption of arsenic (mg As(V)/g_{resin} min), and k_2 is the rate constant of sorption (g_{resin}/mg min). Fig. 7 presents the pseudo-second order curves for arsenic sorption using the nanocomposite PVbNMDG resins. A good agreement between the experimental data and the model was found across the whole time period investigated. In addition, the slopes for the experiments carried out at low initial arsenic concentrations (5.6 and 6.6 mg/L) were very different compared from the rest of the experiments. Pseudo-second order model rate parameters are summarised in Table 1. Correlation coefficients confirmed the excellent fit for all experimental conditions used (initial arsenic concentration and pH) and the calculated sorption capacities were very similar to those values obtained experimentally. In the case of rate constants, it was observed that as the concentration increased, the rate constant decreased. The rate constant for the arsenic concentration of 5.6 mg/L was substantially higher compared with the other values, in agreement with previous observations. These results suggested that the best performance could be achieved using low arsenic concentrations at pH 6.

The relationship between time and the amount of arsenate sorption is important from an engineering perspective. Eq. (5) can be written as follows:

$$t_x = \frac{W}{k_2 q_e} \tag{5}$$

where $W = X/(1 - X)$ and X represents the fractional sorption (q_t/q_e). Thus, as the system approaches equilibrium, $X \to 1$, $W \to \infty$ and $t_x \to \infty$.

Table 2 shows the time needed for different sorption ratios according to rate parameters obtained from the pseudo-second order model. The model predicts a high efficiency for arsenic sorption in experiments carried out at low initial concentrations of arsenic and at pH 6. Specifically, after 1 h of contact more than 90% of the arsenic was removed by the nanocomposite (for experiments carried out at 5.6 and 49.7 mg/L, pH 6).

3.4. Sorption mechanism

Although the models described above provide useful information on the sorption process, they cannot predict the rate-limiting step of the arsenate sorption or provide information on the mechanism. In a heterogeneous process, such as the sorption of arsenic by nanocomposite resins, three consecutive steps can represent the solute transfer: (1) transport of the arsenate anions from the bulk solution through the liquid film surrounding the external surface of the nanocomposite particle (film diffusion), (2) arsenate diffusion into the pores of nanocomposite resins (intra-particle diffusion), and (3) reaction of arsenate (sorption) at interior surface pores and capillary areas of the nanocomposite particle (chemical reaction). The rate of sorption will be controlled by the slowest step, which usually corresponds to film diffusion or intra-particle

Table 2
Relationship of sorption ratio and time.

X	t_x [h] – pH 3			t_x [h] – pH 6		
	6.6 (mg/L)	71.5 (mg/L)	199.6 (mg/L)	5.6 (mg/L)	49.7 (mg/L)	168.9 (mg/L)
0.3	0.4	0.1	0.1	0.04	0.04	0.1
0.5	0.9	0.3	0.3	0.3	0.1	0.2
0.7	2.0	0.7	0.7	0.2	0.2	0.4
0.9	7.9	2.7	2.6	0.8	0.9	1.6
0.95	16.7	5.6	5.5	1.6	1.9	3.5
0.99	86.9	29.4	28.4	8.5	10.1	18.1

diffusion. Film diffusion often controls the rate when the sorption system used has poor mixing, a low concentration of arsenic, a small particle size and a high affinity of the solute for the nanocomposite. On the other hand, intra-particle diffusion will be predominant in systems with a high concentration of solute, good mixing, a large particle size and a low affinity between the adsorbate and the adsorbent [27]. However, due to the characteristics of the adsorbent and the experimental conditions used in the experiment, it is possible to observe both mechanisms acting during arsenic uptake. To elucidate the mechanism of sorption of arsenic by the PVbNMDG nanocomposite, the intra-particle diffusion model was fitted to the experimental data. The model can thus be described by the following equation:

$$q_t = k_{ip} t^{0.5} + C \tag{6}$$

where k_{ip} ($mg/g_{resin}\ min^{0.5}$) corresponds to the rate constant for intra-particle diffusion and C (mg/g_{resin}) is related to the extent of the boundary layer thickness. In an ideal intra-particle diffusion process, a plot of q_t vs. $t^{0.5}$ should give a straight line passing through the origin, otherwise when the intercept is not zero, some degree of external film mass transfer or boundary layer control exists. The larger the intercept, the greater the layer effect [28].

Fig. 8 presents the intra-particle diffusion curves for the sorption of arsenate at pH 3 and 6 and different concentrations. It was observed that curves had multi-linearity, except for low initial concentrations of arsenic (Fig. 8a), which saw gradual increases of q_t with time. In the case of higher concentrations (Fig. 8b and c), multi-linearity was more evident. Multi-linearity has been reported before and two or three steps often appear [29–31]; the first step can be associated to a fast sorption of solute; the second step to a gradual sorption where intra-particle diffusion controls the process. The third step is typically associated with equilibria in which the solute slowly moves within the particle (through micropores).

In this study, two stages of sorption were well distinguished, suggesting that both surface and intra-particle sorption were occurring. The initial linear segment might be associated with surface adsorption, while the final segment of the curve was related to intra-particle diffusion. To elucidate the sorption mechanism associated with each segment of the curve, the intra-particle diffusion model was evaluated for each segment. Table 3 summarises the rate constant and intercept values obtained for linear segments of experimental data (Fig. 8). The correlation coefficients showed that the intra-particle model fit the first step of the sorption better than the second step. The second step began approximately 4 h after contact, where retentions were above 95% and 90% for pH 6 and 3, respectively. This suggested that the second segment corresponded to diffusion of arsenate at interior pores within the nanocomposite with little change in sorption. Taking into account the latter assumption, the first stage should correspond to intra-particle diffusion of arsenate anions into the pores closer to the surface of the nanocomposite particles. The rate constant values increased

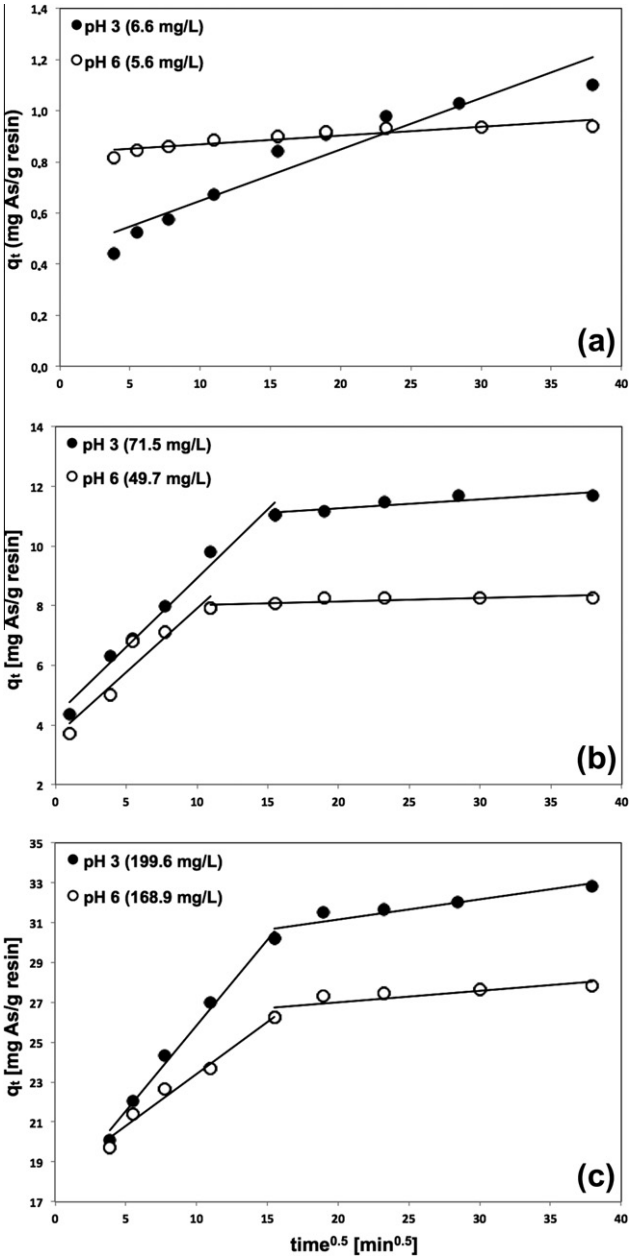

Fig. 8. Intra-particle diffusion plots for arsenic sorption.

with initial arsenic concentration, which could be explained considering that as the initial concentration increased, the concentration gradient was higher, inducing faster diffusion and sorption. For the intercepts, the values were related to the effect of the boundary layer on the adsorbent particle surface, and their magnitude was a measure of rapid adsorption occurring in a short period of time.

According to the results obtained above, the model suggested that both intra-particle and film diffusion mechanisms (at a very early stage) were participating in the sorption process. To confirm the actual stage involved, the experimental data were evaluated using the Boyd relationship developed for a diffusion process in and through an adsorbent particle spherical of radius "r" [32]. The equation is given by:

$$\left(1 - \frac{q_t}{q_e}\right) = \frac{6}{\pi^2} \exp\left(\frac{-D_p \pi^2}{r^2} t\right) \tag{7}$$

Table 3
Intra-particle diffusion constants for different sorption intervals.

As(V) (mg/L)	1st segment			2nd segment		
	k_{ip} (mg As(V)/g_{resin} $min^{0.5}$)	C (mg As(V)/g_{resin})	r^2	k_{ip} (mg As(V)/g_{resin} $min^{0.5}$)	C (mg As(V)/g_{resin})	r^2
5.6[a]	0.0034	0.833	0.8142	–	–	–
6.6[a]	0.0201	0.446	0.9183	–	–	–
49.7	0.434	3.378	0.9827	0.012	7.897	0.5959
71.5	0.462	4.301	0.9801	0.030	10.658	0.8186
168.9	0.521	18.202	0.9742	0.058	25.845	0.6768
199.6	0.888	25.845	0.9887	0.101	29.126	0.8579

[a] These experiments did not present multi-linearity, then the single segment was evaluated.

where q_t and q_e are the arsenic sorption at time t and equilibrium, D_p corresponds to the internal diffusion coefficient (cm^2/min), and r is the radius of the nanocomposite particle. If we consider

$$B = \frac{D_p \pi^2}{r^2} \tag{8}$$

Eq. (7) can rewritten as:

$$Bt = -0.4997 - \ln\left(1 - \frac{q_t}{q_e}\right) \tag{9}$$

From Eq. (9) it is possible to obtain Bt values for each initial concentration. The linearity of a plot of Bt vs. t then provides useful information for distinguishing if external transport or intra-particle diffusion controls the rate of arsenic sorption. The plot should give a straight line passing through the origin if the controlling process is pore diffusion; otherwise, the controlling step is film diffusion.

Fig. 9 shows the Bt curves for different initial arsenic concentrations. The plots were found to have a good correlation at an early stage of sorption, but the curves did not pass through the origin. This suggested that arsenic sorption in this study was governed by external mass transfer (film diffusion). The values of the intercepts for experiments carried out at pH 6 were 1.52, 1.02 and 0.90 for 5.6, 49.7 and 168.9 mg/L of arsenic. In addition, the Bt values at t = 0 moved closer to 0 as the initial arsenic concentration increased. This suggested that as the initial concentration increased, the higher the effect of external mass transfer [31]. The calculated B values were then used to determine the pore diffusion coefficient using Eq. (8). Assuming that nanocomposite particles are spherical and using the mean particle size used for sorption experiments (215 μm), the D_p values for the experiments carried out at pH 6 were 1.37×10^{-10}, 2.63×10^{-10} and 1.60×10^{-10} cm^2/min for 5.6, 49.7 and 168.9 mg As/L.

3.5. Adsorption isotherms

Equilibrium sorption isotherms are one of the most important studies to design adsorption processes. Moreover, isotherms provide useful information on the interaction between the adsorbate and the adsorbent. From adsorption isotherms, it is possible to determine thermodynamic parameters as the experiments are carried out at different temperatures. Equilibrium experiments were thus carried out at 303, 313 and 323 K, and the experimental data were fitted to several isotherm models (Langmuir [33], Freundlich [34], and Dubinin–Radushkevitch (D–R) [35]).

Langmuir equation:

$$\frac{C_e}{q_e} = \frac{1}{k_L q_m} + \frac{C_e}{q_m} \tag{10}$$

Freundlich equation:

$$\log(q_e) = \log(k_F) + \frac{1}{n}\log(C_e) \tag{11}$$

where q_e is the equilibrium sorption of arsenic by the nanocomposite (mg/g_{resin}), C_e is the concentration at equilibrium (mg/L), q_m is the monolayer capacity (mg/g_{resin}), and k_L is the Langmuir constant (L/mg), which is related to the free energy of sorption. For the Freundlich isotherm, k_F is the Freundlich constant and is related to the sorption efficiency, and n is a dimensionless variable indicative of favourability of sorption. The Dubinin–Radushkevitch (D–R) isotherm, which is based on the Polanyi theory, was applied to understand the mechanism involved in arsenic sorption by the PVbNMDG nanocomposite. The linear form of a D–R isotherm is given below:

$$\ln(q_e) = \ln(q_m) + k_{DR}\varepsilon^2 \tag{12}$$

where q_e is the amount of arsenic adsorbed per unit weight of the resin (mg As/g_{resin}), q_m is the adsorption capacity (mg As/g_{resin}), k_{DR} is a constant related to the adsorption energy (mol^2/J^2), and ε is the Polanyi potential, equal to:

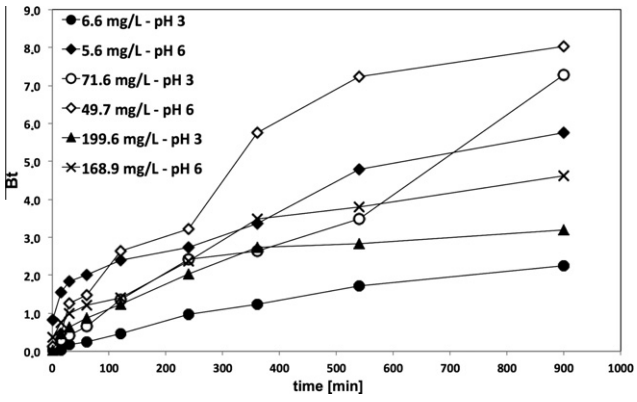

Fig. 9. Boyd plot for arsenic sorption.

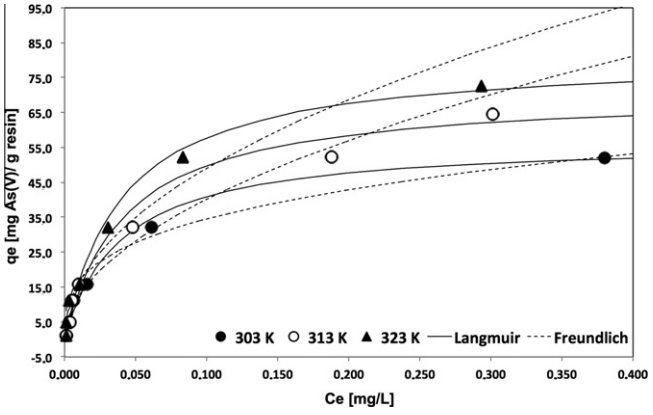

Fig. 10. Adsorption isotherms for As(V) sorption on PVbNMDG nanocomposite.

Table 4
Parameters of Langmuir, Freundlich and Dubinin–Radushkevitch isotherms for arsenic sorption at different temperatures.

T (K)	Langmuir			Freundlich			D–R			
	q_m (mg/g$_{resin}$)	k_L (L/mg)	r^2	n	k_F (mg/g$_{resin}$)	r^2	k_{DR} (mol^2/J^2)	q_m (mg/g$_{resin}$)	E (kJ/mol)	r^2
303	72.26	15.33	0.9962	2.55	70.87	0.9368	1.00×10^{-8}	70.09	7.07	0.9719
313	72.99	19.57	0.9756	1.96	129.71	0.9279	1.01×10^{-8}	81.59	7.02	0.9687
323	82.64	24.2	0.9673	2.05	150.55	0.9625	8.01×10^{-9}	73.53	7.90	0.9746

$$\varepsilon = RT \ln\left(1 + \frac{1}{C_e}\right) \tag{13}$$

where R is the gas constant (J/mol K), T the temperature (K) and C_e the equilibrium concentration of arsenic (mg As/L).

Fig. 10 shows the isotherm obtained for arsenic sorption by PVbNMDG resin at different temperatures. As temperature increased, the sorption capacity also increased, possibly due to high motion of arsenate ions increasing encounters with active sites on the resin. The figure also shows the curves for Langmuir and Freundlich isotherm models. It was observed that the Langmuir described the experimental data well, while the Freundlich isotherm did not.

Table 4 summarises the isotherm parameters associated with each isotherm model evaluated. The correlation coefficients revealed that the Langmuir isotherm fits the experimental data better. The values of the monolayer capacities indicated that as the temperature increased, the adsorption capacity increased. The same trend was observed for the Langmuir constants, suggesting that arsenic sorption by PVbNMDG was an endothermic process.

To confirm the favourability of the arsenic sorption process, the separation factor (R_L) was calculated using the following equation.

$$R_L = \frac{1}{1 + k_L C_0} \tag{14}$$

where R_L is a dimensionless separation factor indicating the efficiency of the adsorption process, K_L is the Langmuir constant and C_0 is the initial adsorbate concentration. The isotherm is (i) unfavourable when $R_L > 1$, (ii) linear when $R_L = 1$, (iii) favourable when $R_L < 1$, and (iv) irreversible when $R_L = 0$. The R_L values calculated for the arsenic concentration of 10 mg/L were 0.0064, 0.0050 and 0.0041 for 303, 313 and 323 K, respectively. These values indicated that arsenic sorption using a PVbNMDG nanocomposite was a favourable process at all temperatures studied.

The Dubinin–Radushkevitch isotherm also presented good agreement with the experimental data, but the correlation coefficients were slightly lower than the Langmuir coefficients. Additionally, the values for sorption capacity did not show the expected trend (the higher the temperature, the higher the sorption capacity) seen in Langmuir.

To evaluate the nature of the interaction between arsenic and the binding sites of *N*-methyl-D-glucamine, the mean free energy of adsorption, E (kJ/mol), defined as the free energy change when one mole of ion is transferred from infinity in solution to the surface of the solid, was calculated from k in Eq. (12) using the following equation:

$$E = (2k_{DR})^{-0.5} \tag{15}$$

The calculated values of E are shown in Table 4. The magnitude of E is useful for estimating the type of sorption involved (i.e., physical, ion exchange or chemisorption). Values of E<8 kJ/mol indicate physical adsorption, while E between 8 and 16 kJ/mol indicates that the adsorption process follows an ion exchange mechanism. A value in the range of 20–40 kJ/mol indicates chemisorption [36–38]. The values of E obtained for arsenic sorption using PVbNMDG resins were in the range of 7–8 kJ/mol, suggesting a physical adsorption of the arsenate anions.

3.6. Thermodynamic parameters

Thermodynamic considerations of an adsorption process are necessary to conclude whether the process is spontaneous or not. The Gibbs free energy change, $\Delta G°$, is an important parameter to evaluate the spontaneity of a process. Reactions occur spontaneously at a given temperature if $\Delta G°$ is a negative quantity. The free energy of arsenic sorption, considering the adsorption equilibrium constant obtained from the Langmuir isotherm, is given by the following equation:

$$\Delta G^0 = -RT \ln(k_L) \tag{16}$$

The thermodynamic parameters $\Delta H°$ and $\Delta S°$ were obtained using the Van't Hoff equation:

$$\log(k_L) = \frac{\Delta S^0}{2.303R} - \frac{\Delta H^0}{2.303RT} \tag{17}$$

A plot of $\log(k_L)$ vs. T then allows the values of $\Delta H°$ and $\Delta S°$ to be determined from the slope and intercept, respectively (Fig. 11). The thermodynamic parameter values obtained at 313 K were −7.50, 18.58 and 0.036 for $\Delta G°$, $\Delta H°$ and $\Delta S°$, respectively. The Gibbs free energy change ($\Delta G°$) value was found to be negative, indicating that arsenic sorption using the PVbNMDG nanocomposites was a feasible and spontaneous process. Moreover, the $\Delta G°$ values became more negative as the temperature increased (−6.88, −7.50, −8.03 kJ/mol for 303, 313, and 323 K). The decrease in the negative value of $\Delta G°$ with an increase in temperature indicated that the adsorption process of arsenic onto PVbNMDG nanocomposite became more favourable at higher temperatures. The enthalpy change ($\Delta H°$) was found to be positive, indicating an endothermic nature for the adsorption. In the case of entropy, a positive entropy change ($\Delta S°$) was found, suggesting an increase in the number of species and hence randomness in the interface sorption process. These results supported the ion exchange nature of the arsenate adsorption mechanism at protonated amines of *N*-methyl-D-glucamine.

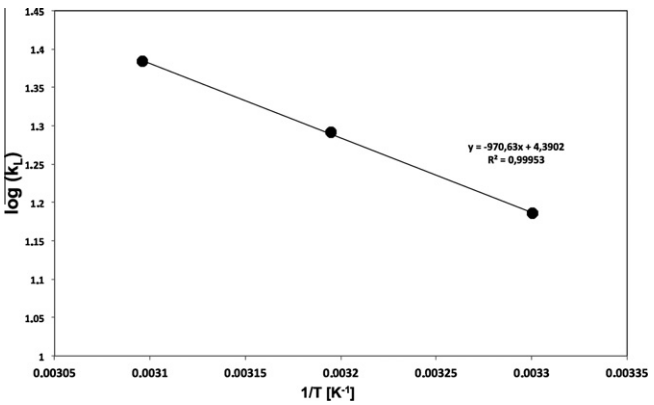

Fig. 11. Van't Hoff relationship of arsenic sorption by PVbNMDG nanocomposite resin.

4. Conclusions

The distribution of the clay sheets in the material presented certain stacking and regularity, verified by X-ray diffraction, indicating the PVbNMDG nanocomposites possessed an intercalated morphology. Arsenic sorption using the PVbNMDG nanocomposites was favoured at a pH where monovalent arsenic species were present (pH 3–6). However, better performance was observed for experiments carried out at pH 6.

The kinetics of arsenic sorption was evaluated as a function of initial concentration and pH, and it was concluded that the best performance could be achieved using low arsenic concentrations at pH 6. Furthermore, arsenic uptake is controlled by film diffusion with a fast and high initial sorption.

The arsenic sorption could be described by the Langmuir isotherm. The nanocomposites presented high arsenic sorption capacity, which increased with temperature. Finally, the calculated thermodynamic parameters showed that arsenic sorption by a PVbNMDG nanocomposite was a spontaneous and endothermic process.

Acknowledgements

The authors thank FONDECYT (Grant No 1110079), PIA (Grant ACT-130), and CIPA. Bruno Urbano thanks CONICYT for Ph.D. financial support and the Graduate Office of the University of Concepción.

References

[1] B.K. Mandal, K.T. Suzuki, Arsenic around the world: a review, Talanta 58 (2002) 201–235.
[2] WHO, Guidelines for Drinking-Water Quality, third ed., World Health Organization, Geneva, 2004.
[3] K.R. Henke, Waste treatment and remediation technologies for arsenic, in: K. Henke (Ed.), Arsenic, John Wiley & Sons Ltd., Chichester, West Sussex, UK, 2009, pp. 351–415.
[4] L.V. Rajakovic, The sorption of arsenic onto activated carbon impregnated with metallic silver and copper, Sep. Sci. Technol. 27 (1992) 1423–1433.
[5] X. Zhu, A. Jyo, Removal of arsenic(V) by zirconium(IV)-loaded phosphoric acid chelating resin, Sep. Sci. Technol. 36 (2001) 3175–3189.
[6] E. Korngold, N. Belayev, L. Aronov, Removal of arsenic from drinking water by anion exchangers, Desalination 141 (2001) 81–84.
[7] J. Kim, M.M. Benjamin, Modeling a novel ion exchange process for arsenic and nitrate removal, Water Res. 38 (2004) 2053–2062.
[8] N. Bıçak, H.O. Ozbelge, L. Yilmaz, B.F. Senkal, Crosslinked polymer gels for boron extraction derived from N-glucidol-N-methyl-2 hydroxypropyl methacrylate, Macromol. Chem. Phys. 201 (2000) 577–584.
[9] N. Kabay, S. Sarp, M. Yuksel, O. Arar, M. Bryjak, Removal of boron from seawater by selective ion exchange resins, React. Funct. Polym. 67 (2007) 1643–1650.
[10] U. Schilde, E. Uhlemann, Separation of several oxoanions with a special chelating resin containing methylamino-glucitol groups, React. Polym. 20 (1993) 181–188.
[11] U. Schilde, H. Kraudelt, E. Uhlemann, Separation of the oxoanions of germanium, tin, arsenic, antimony, tellurium, molybdenum and tungsten with a special chelating resin containing methylaminoglucitol groups, React. Polym. 22 (1994) 101–106.
[12] L. Dambies, R. Salinaro, S. Alexandratos, Immobilized N-methyl-D-glucamine as an arsenate-selective resin, Environ. Sci. Technol. 38 (2004) 6139–6146.
[13] Y.-T. Wei, Y.-M. Zheng, J. Paul Chen, Enhanced adsorption of arsenate onto a natural polymer-based sorbent by surface atom transfer radical polymerization, J. Colloid Interf. Sci. 356 (2011) 234–239.
[14] L. Cumbal, A.K. SenGupta, Arsenic removal using polymer-supported hydrated iron(III) oxide nanoparticles: a role of donnan membrane effect, Environ. Sci. Technol. 39 (2005) 6508–6515.
[15] F. Luo, K. Inoue, The removal of fluoride ion by using metal(III)-loaded amberlite resins, Solvent Extr. Ion Exch. 22 (2004) 305–322.
[16] M. Streat, F.L.D. Cloete, Ion exchange, in: R.W. Rousseau (Ed.), Handbook of Separation Process and Technology, John Wiley & Sons Inc., 1987, pp. 726–729.
[17] N. Kabay, J.L. Cortina, A. Trochimczuk, M. Streat, Solvent-impregnated resins (SIRs) – methods of preparation and their applications, React. Funct. Polym. 70 (2010) 484–496.
[18] B. Urbano, B. Rivas, Poly(sodium 4-styrene sulfonate) and poly(2-acrylamidoglycolic acid) nanocomposite hydrogels: montmorillonite effect on water absorption, thermal, and rheological properties, Polym. Bull. (2011), http://dx.doi.org/10.1007/s00289-00011-00511-00282.
[19] Y.S. Ho, J.C.Y. Ng, G. McKay, Kinetics of pollutant soprtion by biosorbents: review, Sep. Purif. Methods 29 (2000) 189–232.
[20] D.A. Clifford, G.L. Ghurye, Metal-oxide adsorption, ion exchange, and coagulation–microfiltration for arsenic removal from water, in: W.T. Frankenberger (Ed.), Environmental Chemistry of Arsenic, Marcel Dekker, Inc., New York, 2002.
[21] Y.S. Ho, G. McKay, The kinetics of sorption of basic dyes from aqueous solution by sphagnum moss peat, Can. J. Chem. Eng. 76 (1998) 822–827.
[22] Y.S. Ho, G. McKay, Pseudo-second order model for sorption processes, Process Biochem. 34 (1999) 451–465.
[23] H.A. Taylor, N. Thon, Kinetics of chemisorption, J. Am. Chem. Soc. 74 (1952) 4169–4173.
[24] Y.-S. Ho, Review of second-order models for adsorption systems, J. Hazard. Mater. B136 (2006) 681–689.
[25] Y.-T. Wei, Y.-M. Zheng, J. Paul Chen, Enhanced adsorption of arsenate onto a natural polymer-based sorbent by surface atom transfer radical polymerization, J. Colloid Interf. Sci. 356 (2011) 234–239.
[26] F.-C. Wu, R.-L. Tseng, R.-S. Juang, Characteristics of Elovich equation used for the analysis of adsorption kinetics in dye-chitosan systems, Chem. Eng. J. 150 (2009) 366–373.
[27] V. Vadivelan, K.V. Kumar, Equilibrium, kinetics, mechanism, and process design for the sorption of methylene blue onto rice husk, J. Colloid Interf. Sci. 286 (2005) 90–100.
[28] F.-C. Wu, R.-L. Tseng, R.-S. Juang, Initial behavior of intraparticle diffusion model used in the description of adsorption kinetics, Chem. Eng. J. 153 (2009) 1–8.
[29] R.R. Sheha, H.H. Someda, Removal of some chelators from aqueous solutions using polymeric ingredients, Chem. Eng. J. 114 (2005) 105–113.
[30] R.-L. Tseng, F.-C. Wu, R.-S. Juang, Pore structure and metal adsorption ability of chitosans prepared from fishery wastes, J. Environ. Sci. Health Part A A34 (1999).
[31] A.E. Ofomaja, Intraparticle diffusion process for lead(II) biosorption onto mansonia wood sawdust, Biosour. Technol. 101 (2010) 5868–5876.
[32] G.E. Boyd, A.W. Adamson, L.S. Myers, The exchange adsorption of ions from aqueous solutions by organic zeolites. II. Kinetics1, J. Am. Chem. Soc. 69 (1947) 2836–2848.
[33] N.Z. Misak, Adsorption isotherms in ion exchange reactions. Further treatments and remarks on the application of the Langmuir isotherm, Colloids Surf. A. 97 (1995) 129–140.
[34] F. Gode, E. Pehlivan, Removal of chromium(III) from aqueous solutions using Lewatit S 100: the effect of pH, time, metal concentration and temperature, J. Hazard. Mater. 136 (2006) 330–337.
[35] N.D. Hutson, R.T. Yang, Theoretical basis for the Dubinin–Radushkevitch (D–R) adsorption isotherm equation, Adsorption 3 (1997) 189–195.
[36] S. Debnath, U.C. Ghosh, Kinetics, isotherm and thermodynamics for Cr(III) and Cr(VI) adsorption from aqueous solutions by crystalline hydrous titanium oxide, J. Chem. Thermodyn. 40 (2008) 67–77.
[37] S. Samatya, N. Kabay, U. Yuksel, M. Arda, M. Yuksel, Removal of nitrate from aqueous solution by nitrate selective ion exchange resins, React. Funct. Polym. 66 (2006) 1206–1214.
[38] P.S. Kumar, S. Ramalingam, S.D. Kirupha, A. Murugesan, T. Vidhyadevi, S. Sivanesan, Adsorption behavior of nickel(II) onto cashew nut shell: equilibrium, thermodynamics, kinetics, mechanism and process design, Chem. Eng. J. 167 (2011) 122–131.